ChemComm

COMMUNICATION

A luminescent ultrathin film with reversible sensing toward pressure†

Mingwan Li, Rui Tian, Dongpeng Yan, Ruizheng Liang,* Min Wei,* David G. Evans and Xue Duan

Cite this: *Chem. Commun.*, 2016, **52**, 4663

Received 10th December 2015, Accepted 26th February 2016

DOI: 10.1039/c5cc10158a

www.rsc.org/chemcomm

A flexible ultrathin film based on alternate assembly of a sodium polyacrylate (PAA) modified styrylbiphenyl derivative (BTBS) and layered double hydroxide nanosheets is fabricated, which exhibits pressure-responsive photoluminescence with a high sensitivity and good reversibility.

Luminescent materials, which respond to environmental stimuli such as temperature, pressure or humidity, are of great interest due to their potential applications in fluorescent switches, information storages and optical devices.[1] Since pressure is one of the most common natural external stimuli, pressure-induced fluorescence sensors with sensitive and stable responses can be used in pressure-sensing and optical-recording systems. However, compared with pH-, light-, and temperature-sensitive materials which are relatively well explored, the study on pressure fluorescence sensors remains inadequate.[2] Recently, great efforts have been devoted to the study of piezochromic powdered materials,[3] but two considerable issues are not well-resolved: (i) the response range of most piezochromic materials is the GPa level and the detection level in MPa is fairly rare; (ii) powdered materials normally suffer from inconveniency in operation and recycling use. Therefore, constructing a convenient and highly sensitive piezochromic material is highly necessary for practical applications.

In the past decades, the incorporation of guest luminescent molecules into a 2D host matrix has attracted much attention since the fluorescence performance and stability of luminescent species can be optimized by the host–guest interactions. Layered double hydroxides (LDHs) with the general formula $[M^{II}_{1-x}M^{III}_{x}(OH)_2]^{z+}A^{n-}_{z/n}\cdot yH_2O$ (M^{II} and M^{III} are di- and trivalent metal cations, respectively, and A^{n-} is a guest anion)[4] are a class of 2D layered host materials which have been widely applied in catalysis, biology, and photofunctional materials.[5] LDH microcrystals can be exfoliated into positively-charged nanosheets as building blocks for ultrathin films (UTFs) used in fluorescence imaging, display and detection.[6–10] As a kind of important luminescent organic species, styrylbiphenyl and its derivatives are widely studied in fluorescent brighteners, light-emitting diodes and magneto-optical sensors owing to their excellent optical and electronic performance.[11] In our previous work, a styrylbiphenyl derivative/LDH powdered material was obtained, which showed piezochromic performance ascribed to the change in its aggregation state.[12] If the non-radiative transition originating from the vibration/rotation state of a luminescent molecule is inhibited by external pressure, its radiative transition would be enhanced with promoted fluorescence performance. This further inspires us to explore the change in the molecular vibration/rotation state of styrylbiphenyl derivatives as a function of external pressure, so as to give a molecular mobility-dependent fluorescence sensor toward pressure.

In this work, we report the fabrication of an organic–inorganic flexible ultrathin film (UTF) system *via* layer-by-layer (LBL) assembly of a sodium polyacrylate (PAA) modified styrylbiphenyl derivative (BTBS, Fig. S1, ESI†) and LDH nanosheets (Scheme 1). The resulting UTF shows a long-range ordered structure, which exhibits a homogeneous surface and uniform blue light emission. More interestingly, the luminescence property of the UTF is sensitive to pressures at the MPa level: gradually enhanced fluorescence

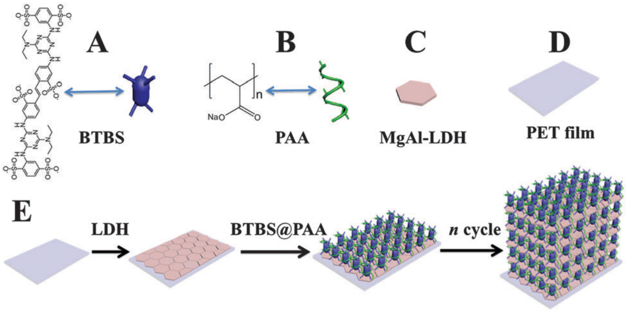

Scheme 1 Schematic illustration for (A) BTBS, (B) PAA, (C) MgAl-LDH nanosheet, (D) PET film, and (E) the assembly process of $(BTBS@PAA/LDH)_n$ UTFs.

State Key Laboratory of Chemical Resource Engineering, Beijing University of Chemical Technology, Box 98, Beijing 100029, P. R. China.
E-mail: liangruizheng2000@163.com, weimin@mail.buct.edu.cn;
Fax: +86 10-6442-5385

† Electronic supplementary information (ESI) available. See DOI: 10.1039/c5cc10158a

is observed along with the increase of pressure, which is attributed to the restrained vibration/rotation of BTBS by the external pressure. In addition, the UTF shows high photostability under UV irradiation. This work provides a facile method for the preparation of pressure-sensitive UTF, which can be used as a promising candidate in pressure sensors and detection.

To fabricate the $(BTBS@PAA/LDH)_n$ UTFs, the BTBS@PAA micelle solution was firstly prepared through mixing BTBS and PAA in deionized water followed by an ultrasonic treatment. Both the absorption peak and fluorescence intensity of BTBS@PAA micelle solution are consistent with those of BTBS, indicating the excellent compatibility of BTBS and PAA (Fig. S2 and S3, ESI†). Isothermal titration calorimetry (ITC) was used to measure the interaction between PAA and BTBS (Fig. S4, ESI†). The negative values of ΔH and $-T\Delta S$ indicate the formation of hydrogen bonding between PAA and BTBS,[13] which facilitates their co-assembly into the gallery of LDH nanosheets. Layer-by-layer assembly was carried out to construct the multilayer $(BTBS@PAA/LDH)_n$ (n = 0–30) UTFs by alternate deposition of BTBS@PAA and LDH nanosheets on the PET substrate, which can be monitored by UV-visible absorption spectroscopy. Absorption bands at ~210, ~272 and ~351 nm are observed (Fig. S2, ESI†), corresponding to the π–π* transition of BTBS. The peak intensity enhances gradually along with the increase of the bilayer number (n), and a linear correlation between the absorbance and n is observed (Fig. 1A), indicating a stepwise and regular film growth procedure. The as-obtained UTFs exhibit high uniformity and transparency (Fig. 1B). The fabrication of multilayer $(BTBS@PAA/LDH)_n$ (n = 0–30) UTFs is also monitored by fluorescence emission spectra. A strong emission at ~450 nm is observed for these UTFs, whose intensity displays a monotonic increase along with the bilayer number n (Fig. 1C). Compared with the emission peak at ~435 nm for the pristine BTBS@PAA solution (Fig. S3, ESI†), the $(BTBS@PAA/LDH)_n$ (n = 0–30) UTFs undergo a red shift of ~15 nm, which can be attributed to the interaction between BTBS@PAA and the LDH nanosheets. The visualisation of these UTFs under UV light irradiation (Fig. 1D) reveals a well-defined blue luminescence with enhanced brightness upon increasing n.

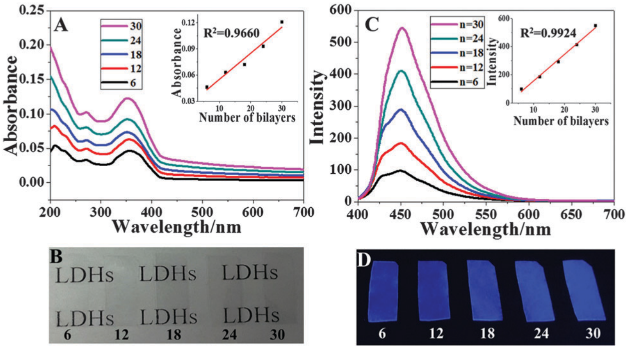

Fig. 1 (A) UV-vis absorption spectra of $(BTBS@PAA/LDH)_n$ (n = 0–30) UTFs (the inset shows the linear correlation between absorbance at 351 nm and bilayer number); (B) photographs of these UTFs under daylight; (C) fluorescence emission spectra of these UTFs (the inset shows the linear correlation between the intensity at 450 nm and bilayer number); (D) photographs of these UTFs under UV light irradiation (365 nm).

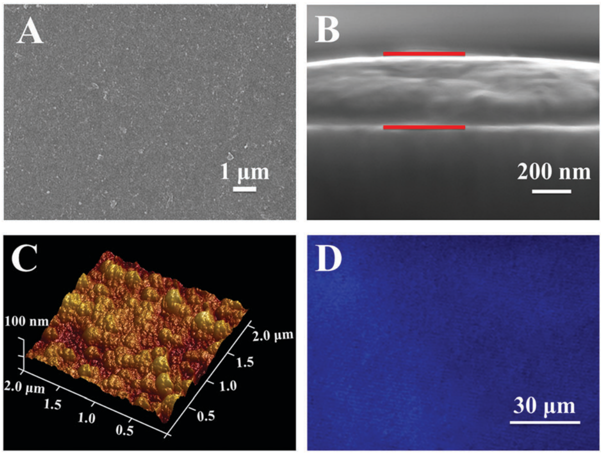

Fig. 2 The structural and morphological characterization of the $(BTBS@PAA/LDH)_{30}$ UTF: (A) top-view SEM image; (B) side-view SEM image; (C) tapping-mode AFM topographical image; and (D) fluorescence microscope image.

The structural and morphological properties of $(BTBS@PAA/LDH)_n$ UTFs were studied. Typical top-view SEM images of these UTFs (Fig. 2A and Fig. S5, ESI†) show a homogeneous surface morphology. Additionally, the thickness of UTFs is estimated based on their side-view SEM images (Fig. 2B and Fig. S6, ESI†), from which an approximately linear increase of film thickness as a function of n is observed. An average thickness increment of 12.60 nm per bilayer cycle is obtained (Table S1, ESI†), which is consistent with the small-angle XRD observations (Table S2, ESI,† 12.46 nm). AFM topographical images (Fig. 2C and Fig. S7, ESI†) show that the root-mean square (RMS) roughness of these UTFs ranges from 2.48 to 10.08 nm (Table S1, ESI†), indicating a continuous and relatively smooth surface. Furthermore, the $(BTBS@PAA/LDH)_n$ UTFs display a homogeneous blue color with strong brightness under a fluorescence microscope (Fig. 2D and Fig. S8, ESI†), which suggests a uniform distribution of BTBS in the UTFs. We further studied the internal structure of $(BTBS@PAA/LDHs)_{30}$ UTFs using a laser scanning confocal microscope, and the results showed that the UTFs emit uniform blue fluorescence from inside to outside (the DVD and Fig. S9, ESI†), indicating the intrinsic homogeneity of whole UTFs.

To investigate the fluorescence response of UTFs toward pressure, we firstly investigated the response time and found that the fluorescence intensity of UTFs can reach a stable state at 10 s toward 10 MPa pressure (Fig. S10, ESI†). The fluorescence emission spectra of the $(BTBS@PAA/LDH)_{30}$ UTF under different pressures (0–12 MPa) are further recorded. As shown in Fig. 3A, the fluorescence intensity of the $(BTBS@PAA/LDH)_{30}$ UTF at ~450 nm increases systematically with enhanced pressure, and the correlation can be fitted by the quadratic equation of pressure: $I/I_0 = -0.0047P^2 + 0.1269P + 0.9996$ (I and I_0 stand for the pressed and initial fluorescence intensity, respectively; P represents the pressure and $R^2 = 0.999$) (Fig. 3B). More importantly, the pressed UTF can recover its original state by simply heating at 70 °C for 5 min. The sensitive and reversible response would guarantee its practical applications. As control samples, the pressure responses

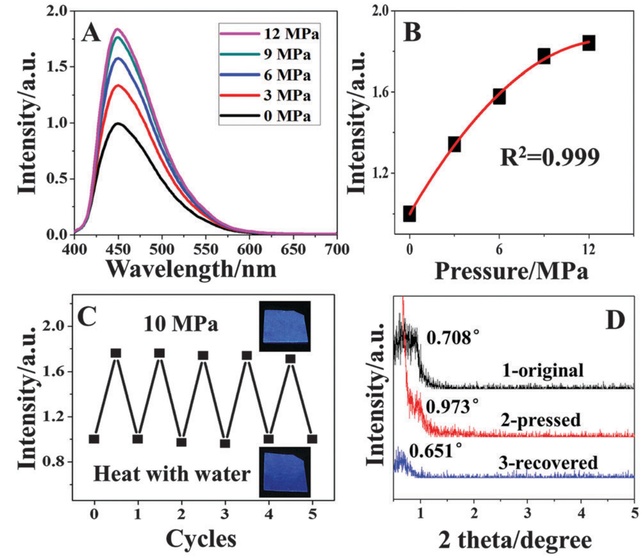

Fig. 3 (A) Fluorescence emission spectra of the $(BTBS@PAA/LDH)_{30}$ UTF in the presence of various external pressures; (B) the correlation between intensity at 450 nm and pressure; (C) reversibility of the fluorescence intensity under two different conditions: 10 MPa and released state; the insets show the corresponding photographs under UV light irradiation (365 nm); (D) the small-angle XRD patterns of this UTF in a cycle: (1) the original state, (2) the pressed state, (3) the recovered state by heating at 70 °C for 5 min.

of the $(BTBS/LDH)_{30}$ film, $(BTBS@PAA/PDDA)_{30}$ film and BTBS@PAA drop-casting film are also studied. The $(BTBS/LDH)_{30}$ film shows a rather insensitive signal; and the $(BTBS@PAA/PDDA)_{30}$ and BTBS@PAA drop-casting films give very slight response (Fig. S11, ESI†). The results indicate that the combination of PAA and LDHs provides a flexible 2D microenvironment which enables the contraction–expansion transformation of the interlayer region toward external pressure.

The excitation-state lifetime of $(BTBS@PAA/LDH)_{30}$ UTF at the original, compressed and recovered state is studied, respectively, and the data are fitted by ternary order. Fig. S12 and Tables S3, S4 (ESI†) show that the fluorescence lifetime of $(BTBS@PAA/LDH)_{30}$ UTF is 0.71 ns. After applying a pressure of 10 MPa for 10 s, the lifetime is promoted to 1.13 ns. After heating at 70 °C for 5 min, the lifetime is recovered to 0.85 ns. Accordingly, the quantum yield (QY) of UTF in the whole compressing–recovering process is improved from 12.82% to 23.15% and then recovered to 13.71% finally. The enhancement in lifetime and QY could be attributed to the inhibited non-radiative transition of BTBS under external pressure. Moreover, the fluorescence recovery of the UTF is easily achieved by heat treatment, and this process shows a good reversibility and repeatability (Fig. 3C).

In order to investigate the reason for the pressure-responsive fluorescence behavior, AFM, FT-IR and small-angle XRD are employed to further detect the morphological and structural changes of the UTF. The surface morphology of $(BTBS@PAA/LDH)_{30}$ UTF displays a reversible change in a compressing–recovering cycle: the RMS roughness changes from 10.08 nm (original) to 4.68 nm (compressed) and finally recovers to 8.21 nm (Fig. S13 and Table S2, ESI†). The decreased interlayer spacing of $(BTBS@PAA/LDH)_{30}$ UTF under external pressure would induce the changes in arrangement, conformation and intermolecular interactions of BTBS, which impose influences on its molecular vibration. Moreover, the vibration/rotation of BTBS in UTFs during this cycle was further investigated by FT-IR. It is found that the stretching vibration intensity at 3430, 2968, 1248 cm^{-1} (assigned to $R_2N–H$, $–CH_3$, C–N of BTBS, respectively) as well as 1097 and 1018 cm^{-1} (assigned to $S{=}O$ of BTBS) decreases obviously under 10 MPa pressure for 10 s. Subsequently, the band intensity recovers the original state *via* heat treatment (Fig. S14, ESI†). FT-IR results definitely demonstrate that the vibration of BTBS is inhibited by external pressure, accounting for the enhanced fluorescence intensity. This sensing principle is different from the formation of J-type aggregation of styrylbiphenyl derivatives in previous work.[12] In addition, the $(BTBS@PAA/LDH)_{30}$ UTF maintains a periodic long-range ordered structure in the whole compressing–recovering process (Fig. 3D). The UTF shows a reflection at $2\theta \sim 0.708°$, corresponding to an interlayer spacing of 12.46 nm (Fig. $3D_1$). After applying a pressure of 10 MPa, the diffraction angle becomes $2\theta \sim 0.973°$, indicating a decreased interlayer spacing of 9.07 nm (Fig. $3D_2$). A further heat treatment induces the recovery to its original state, with $2\theta \sim 0.651°$ and a released interlayer spacing of 13.55 nm (Fig. $3D_3$). The thickness of UTF also undergoes a contraction–expansion cycle: from 373.8 nm to 272.1 nm and then back to 406.5 nm (Table S2, ESI†). The decreased interlayer spacing of $(BTBS@PAA/LDH)_{30}$ UTF under external pressure would produce a constringent configuration of BTBS with depressed vibration/rotation, which reduces its non-radiative transition, accounting for the promoted fluorescence intensity, lifetime and QY as discussed above; the following release of interlayer spacing leads to the recovery of BTBS to its original configuration state.

UV-resistance capability is a key factor for practical applications of luminescent films. To study the photostability of $(BTBS@PAA/LDH)_{30}$ UTF, it is irradiated by UV light (365 nm) for a period of time, with the $(BTBS@PAA/PDDA)_{30}$ film and the drop-casting BTBS@PAA film as control samples. During the 0–300 min irradiation, the fluorescence intensity of $(BTBS@PAA/LDH)_{30}$ UTF decreases gradually and reaches a steady value after 210 min; while continuous decline is observed for the $(BTBS@PAA/PDDA)_{30}$ and drop-casting BTBS@PAA films. After 300 min, the fluorescence intensity of $(BTBS@PAA/LDH)_{30}$ UTF decreases to 64.0% of its original value; in contrast, only 47.9% and 29.1% are maintained for the $(BTBS@PAA/PDDA)_{30}$ and BTBS@PAA films, respectively (Fig. S15, ESI†). The results demonstrate that the UV resistance capability of BTBS is significantly enhanced within the 2D inorganic LDH matrix.

In summary, flexible and long-range ordered $(BTBS@PAA/LDH)_n$ UTFs with blue fluorescence have been constructed by an LBL assembly technique. The fluorescence intensity of the UTF at ~450 nm enhances systematically as the external pressure increases, accompanied by improved lifetime and QY; a further heat treatment induces the recovery of UTF to its initial state. Reversible structural and morphological changes are also observed during this compressing–recovering cycle. The piezochromic behavior of $(BTBS@PAA/LDH)_{30}$ UTF can be attributed to the inhibited vibration/rotation of BTBS with applied external pressure. In addition, the photostability of $(BTBS@PAA/LDH)_{30}$ UTF is promoted markedly, which can be potentially used in pressure-sensing and optical-recording systems.

This work was supported by the 973 Program (Grant No. 2014CB932103), the National Natural Science Foundation of China (NSFC), the Fundamental Research Funds for the Central Universities (YS 1406). M. Wei appreciates the financial aid from the China National Funds for Distinguished Young Scientists of the NSFC.

Notes and references

1 (*a*) M. Irie, T. Fukaminato, T. Sasaki, N. Tamai and T. Kawai, *Nature*, 2002, **420**, 759; (*b*) F. Galindo, J. C. Lima, S. V. Luis, M. J. Melo, A. J. Parola and F. Pina, *J. Mater. Chem.*, 2005, **15**, 2840; (*c*) L. Jin, Y. Fang, P. Hu, Y. Zhai, E. Wang and S. Dong, *Chem. Commun.*, 2012, **48**, 2101; (*d*) H. Shi, J. Dai, L. Shi, M. Wang, L. Fang, S. Shuang and C. Dong, *Chem. Commun.*, 2012, **48**, 8586.

2 (*a*) P. T. Snee, R. C. Somers, G. Nair, J. P. Zimmer, M. G. Bawendi and D. G. Nocera, *J. Am. Chem. Soc.*, 2006, **128**, 13320; (*b*) X. Cui, J. Zhao, Y. Zhou, J. Ma and Y. Zhao, *J. Am. Chem. Soc.*, 2014, **136**, 9256; (*c*) S. Helmy, F. A. Leibfarth, S. Oh, J. E. Poelma, C. J. Hawker and J. R. d. Alaniz, *J. Am. Chem. Soc.*, 2014, **136**, 8169; (*d*) A. Sedlmeier, D. E. Achatz, L. H. Fischer, H. H. Gorris and O. S. Wolfbeis, *Nanoscale*, 2012, **4**, 7090; (*e*) F. Ye, C. Wu, Y. Jin, Y. H. Chan, X. Zhang and D. T. Chiu, *J. Am. Chem. Soc.*, 2011, **133**, 8146.

3 Y. Dong, B. Xu, J. Zhang, X. Tan, L. Wang, J. Chen, H. Lv, S. Wen, B. Li, L. Ye, B. Zou and W. Tian, *Angew. Chem., Int. Ed.*, 2012, **51**, 10782.

4 (*a*) S. Gago, T. Costa, J. S. d. Melo, I. S. Goncalves and M. Pillinger, *J. Mater. Chem.*, 2008, **18**, 894; (*b*) S. Gago, M. Pillinger, R. A. S. Ferreira, L. D. Carlos, T. M. Santos and I. S. Goncalves, *Chem. Mater.*, 2005, **17**, 5803; (*c*) X. Q. Hou and R. J. Kirkpatrick, *Inorg. Chem.*, 2001, **40**, 6397; (*d*) B. Monteiro, S. Gago, F. A. A. Paz, R. Bilsborrow, I. S. Goncalves and M. Pillinger, *Inorg. Chem.*, 2008, **47**, 8674; (*e*) M. C. Richardson and P. S. Braterman, *J. Phys. Chem. C*, 2007, **111**, 4209; (*f*) J. Y. Uan, J. K. Lin and Y. S. Tung, *J. Mater. Chem.*, 2010, **20**, 761.

5 (*a*) C. A. Antonyraj, P. Koilraj and S. Kannan, *Chem. Commun.*, 2010, **46**, 1902; (*b*) A. M. Fogg, A. J. Freij and G. M. Parkinson, *Chem. Mater.*, 2002, **14**, 232; (*c*) A. I. Khan, L. X. Lei, A. J. Norquist and D. O'Hare, *Chem. Commun.*, 2001, 2342; (*d*) F. Leroux and J. P. Besse, *Chem. Mater.*, 2001, **13**, 3507; (*e*) G. M. Lombardo, G. C. Pappalardo, F. Costantino, U. Costantino and M. Sisani, *Chem. Mater.*, 2008, **20**, 5585.

6 (*a*) Q. Wang and D. O'Hare, *Chem. Rev.*, 2012, **112**, 4124; (*b*) L. Desigaux, M. B. Belkacem, P. Richard, J. Cellier, P. Léone, L. Cario, F. Leroux, C. Taviot-Guého and B. Pitard, *Nano Lett.*, 2006, **6**, 199; (*c*) F. Leroux and C. Taviot-Gueho, *J. Mater. Chem.*, 2005, **15**, 3628; (*d*) G. R. Williams, A. M. Fogg, J. Sloan, C. Taviot-Gueho and D. O'Hare, *Dalton Trans.*, 2007, 3499; (*e*) G. R. Williams and D. O'Hare, *J. Mater. Chem.*, 2006, **16**, 3065.

7 (*a*) D. Chen, S. Huang, C. Zhang, W. Wang and T. Liu, *Thin Solid Films*, 2010, **518**, 7081; (*b*) E. Coronado, C. Marti-Gastaldo, E. Navarro-Moratalla, A. Ribera and S. Tatay, *Inorg. Chem.*, 2013, **52**, 6214; (*c*) S. Huang, X. Cen, H. Peng, S. Guo, W. Wang and T. Liu, *J. Phys. Chem. B*, 2009, **113**, 15225; (*d*) D. Yan, J. Lu, L. Chen, S. Qin, J. Ma, M. Wei, D. G. Evans and X. Duan, *Chem. Commun.*, 2010, **46**, 5912.

8 R. Liang, M. Wei, D. G. Evans and X. Duan, *Chem. Commun.*, 2014, **50**, 14071.

9 R. Liang, S. Xu, D. Yan, W. Shi, R. Tian, H. Yan, M. Wei, D. G. Evans and X. Duan, *Adv. Funct. Mater.*, 2012, **22**, 4940.

10 W. Shi, S. He, M. Wei, D. G. Evans and X. Duan, *Adv. Funct. Mater.*, 2010, **20**, 3856.

11 (*a*) A. Ajayaghosh and V. K. Praveen, *Acc. Chem. Res.*, 2007, **40**, 644; (*b*) F. Gao, Q. Liao, Z. Xu, Y. Yue, Q. Wang, H. Zhang and H. Fu, *Angew. Chem., Int. Ed.*, 2010, **49**, 732.

12 D. Yan, J. Lu, J. Ma, S. Qin, M. Wei, D. G. Evans and X. Duan, *Angew. Chem., Int. Ed.*, 2011, **50**, 7037.

13 (*a*) J. Li, R. Guo, J. Shen, T. Yang and Z. Yin, *Small*, 2014, **10**, 1351; (*b*) Z. Yin, J. Shen, R. Gropeanu, G. O. Pflugfelder, T. Weil and K. Mullen, *Small*, 2008, **4**, 894.